Retrospective Study

Using Artificial Intelligence to Predict Residual Distal Lumbosacral Pain Post Percutaneous Kyphoplasty for Osteoporotic Vertebral Compression Fractures

Yuye Zhang, MD[1], Yingzi Zhang, MD[1], Xingyu You, MD[2], Xueli Qiu, MD[1], Wenxiang Tang, MD[1], Yufei Zhang, MD[1], and Fanguo Lin, MD[1]

From: [1]Department of Orthopedics, The Second Affiliated Hospital of Soochow University, Suzhou, People's Republic of China; [2]Department of Computer Science and Mathematics, Arcadia University, Glenside, PA.

Address Correspondence: Fanguo Lin, MD Department of Orthopedics, The Second Affiliated Hospital of Soochow University, No. 1055, Sanxiang Road, Suzhou, People's Republic of China. E-mail: fancoolin@163.com

Disclaimer: This work was supported by the Science and Education Strong Health Project of Suzhou in the People's Republic of China (No. MSXM2024011).

Conflict of interest: Each author certifies that he or she, or a member of his or her immediate family, has no commercial association (i.e., consultancies, stock ownership, equity interest, patent/licensing arrangements, etc.) that might pose a conflict of interest in connection with the submitted article.

Contributors: All authors contributed significantly to the planning, conduct, and reporting of the work described in this paper. Yuye Zhang, Yingzi Zhang, Xingyu You, and Xueli Qiu contributed equally to this paper. Yuye Zhang, Yingzi Zhang, Xingyu You, and Xueli Qiu are joint first authors.

Article received: 12-14-2024
Revised article received: 01-03-2025
Accepted for publication: 03-05-2025

Free full article: www.painphysicianjournal.com

Background: Percutaneous kyphoplasty (PKP) can restore spinal stability and relieve pain in patients with osteoporotic vertebral compression fractures (OVCF). However, in some cases, distal lumbosacral pain (DLP) persists postoperatively, affecting patients' expectations of the surgery and their recovery to activities of daily life.

Objective: To use artificial intelligence to predict DLP post-PKP for OVCF, thereby providing personalized treatment plans for patients with OVCF.

Study Design: Retrospective study.

Setting: The study was carried out at a university hospital.

Methods: A univariate analysis was performed to identify the risk factors for DLP post-PKP. A heatmap analysis was conducted to examine the relationships between variables in the dataset. A random forest model was established, and its performance was evaluated using a confusion matrix. After validating and tuning the model, features were ranked based on their contribution to prediction accuracy.

Results: A total of 179 patients completed this study. Patients were divided into 2 groups (Group 0 without DLP; Group 1 with DLP). The univariate analysis indicated statistically significant differences in terms of bone density, intravertebral vacuum cleft, sarcopenia, bone cement distribution, interspinous ligament degeneration, and Hounsfield unit ($P < 0.05$). The heatmap analysis revealed a moderate correlation between DLP and both sarcopenia and interspinous ligament degeneration. A random forest model was built. The confusion matrix showed that the model exhibited strong performance across all metrics. The random forest model showed that the preoperative Cobb angle and sarcopenia were the most critical features.

Limitations: This was a retrospective study, which may be prone to selection and recall bias. Single-center noncontrolled studies may also introduce bias.

Conclusion: Our random forest model can effectively predict DLP post-PKP for OVCF, assisting in the selection of treatment plans.

Key words: Artificial intelligence, osteoporotic vertebral compression fracture, percutaneous kyphoplasty, distal lumbosacral pain

Ethics approval: Ethics Committee of Second Affiliated Hospital of Soochow University.

Pain Physician 2025: 28:E337-E346

Osteoporotic vertebral compression fractures (OVCF) are common. They mainly present as localized pain at the fracture site or as distal lumbosacral pain (DLP). Percutaneous kyphoplasty (PKP) is an effective treatment for OVCF. It can alleviate pain caused by OVCF and significantly reduce the mortality rate of patients (1-3). However, in some patients, DLP is not completely relieved by surgery. Persistent DLP leads to a loss of confidence in the surgery and affects the patient's quality of life (4-6).

Studies have found that combining a facet joint block or steroid injections with PKP can effectively reduce the incidence of postoperative DLP in patients with OVCF (7,8). However, not all patients with OVCF experience postsurgical DLP. Therefore, it is particularly important to accurately predict whether patients with OVCF will have postoperative DLP and to provide precise early intervention.

Previous studies have explored risk factors and prediction models for DLP post-OVCF surgery, but these studies only assessed which factors may influence postoperative DLP (9-11). No research has been conducted on the importance scores of various risk factors or their roles in residual postoperative DLP.

Artificial Intelligence (AI) has rapidly advanced recently. It shows great potential in imaging analysis, disease diagnosis, and personalized treatment. AI can integrate various clinical information from patients to analyze disease-related risk factors, thereby optimizing diagnostic processes and quickly and accurately predicting the occurrence of related diseases (12-14). The main objective of our study was to build a random forest model based on the clinical data of patients with OVCF. This model was designed to evaluate the role of various factors in postsurgical DLP and provide importance scores. It aims to accurately predict whether patients with OVCF will experience postoperative DLP, ultimately leading to precise and personalized treatment for these patients.

Methods

Patient Population

This is a retrospective study; it was reviewed and approved by the Ethics Committee of Second Affiliated Hospital of Soochow University, People's Republic of China. Patients with OVCF who were admitted to our hospital and underwent surgical treatment from January 2021 through December 2023 were enrolled. After admission, all patients underwent spinal anteroposterior and lateral x-rays, computed tomography, and magnetic resonance imaging.

The inclusion criteria were: 1) clearly diagnosed single-level thoracolumbar OVCF (T10-L2); 2) no symptoms of spinal cord or nerve compression; 3) preoperative pain with a Visual Analog Scale (VAS) pain score of ≥ 5; 4) previous PKP; and 5) complete postoperative outpatient follow-up data.

The exclusion criteria were: 1) thoracolumbar fractures caused by severe trauma, such as car accidents or high falls; 2) spinal tumors; or 3) spinal tuberculosis.

When enrolled, each patient's preoperative general conditions were recorded, including gender; age; fracture segment; body mass index; bone mineral density (BMD); diagnosed hypertension and/or diabetes time from fracture to surgery; posterior fascia oedema (PFO); intravertebral vacuum cleft (IVC); sarcopenia;, preoperative VAS score; preoperative Oswestry Disability Index (ODI) score; interspinous ligament degeneration (ISLD); preoperative Cobb angle; preoperative anterior vertebral height (AVH); and Hounsfield Unit (HU) values.

Surgical Techniques

With the patient prone and under general anesthesia, a puncture needle was inserted under C-arm fluoroscopy. A working cannula was then inserted, followed by placing a balloon filled with contrast medium into the appropriate position. The balloon was expanded to restore the vertebra. Once the bone cement reached the late stringy phase, it was injected through bilateral working cannulas under C-arm guidance.

Postoperative Management and Follow-Up

All enrolled patients successfully completed the surgery and received postoperative anti-osteoporosis treatment. On the first postoperative day, thoracolumbar x-rays were taken to assess vertebral repositioning, bone cement dispersion, and bone cement leakage. The VAS score for DLP and the ODI score were also evaluated on the first postoperative day. Data measurements were conducted by 3 spine surgeons, each with more than 5 years of experience. The surgeons were blinded to the patient's group information before measurement to assure a double-blind process; the final value was taken as the average of the 3 surgeons' measurements. Additionally, VAS and ODI scores for DLP were collected during outpatient follow-ups at one month and 3 months postoperatively.

Data Measurement Methods

IVC

Computed tomography scans were performed to observe for the vacuum sign within the vertebral body (Fig. 1A).

PFO

The lumbar region was evaluated with magnetic resonance imaging, looking for linear or patchy high signal areas in the subcutaneous and fascial layers (Fig. 1B).

ISLD

Magnetic resonance imaging was used to examine the interspinous ligament for high signals on fat-suppressed T2-weighted images (Fig. 1C).

Bone Cement Distribution

Good bone cement distribution was determined by seeing an even spread throughout the vertebra as seen on anteroposterior and lateral x-ray views, with diffusion into both the upper and lower endplates. Poor distribution appeared as clumped bone cement localized to specific areas within the vertebra as seen on x-rays (Figs. 1D, 1E).

Bone Cement Leakage

Leakage was defined as the presence of bone cement outside the vertebra as seen on anteroposterior or lateral x-rays (Fig. 1F).

Sarcopenia

We measured the cross-sectional area of the psoas muscle at the level of L3 on computed tomography im-

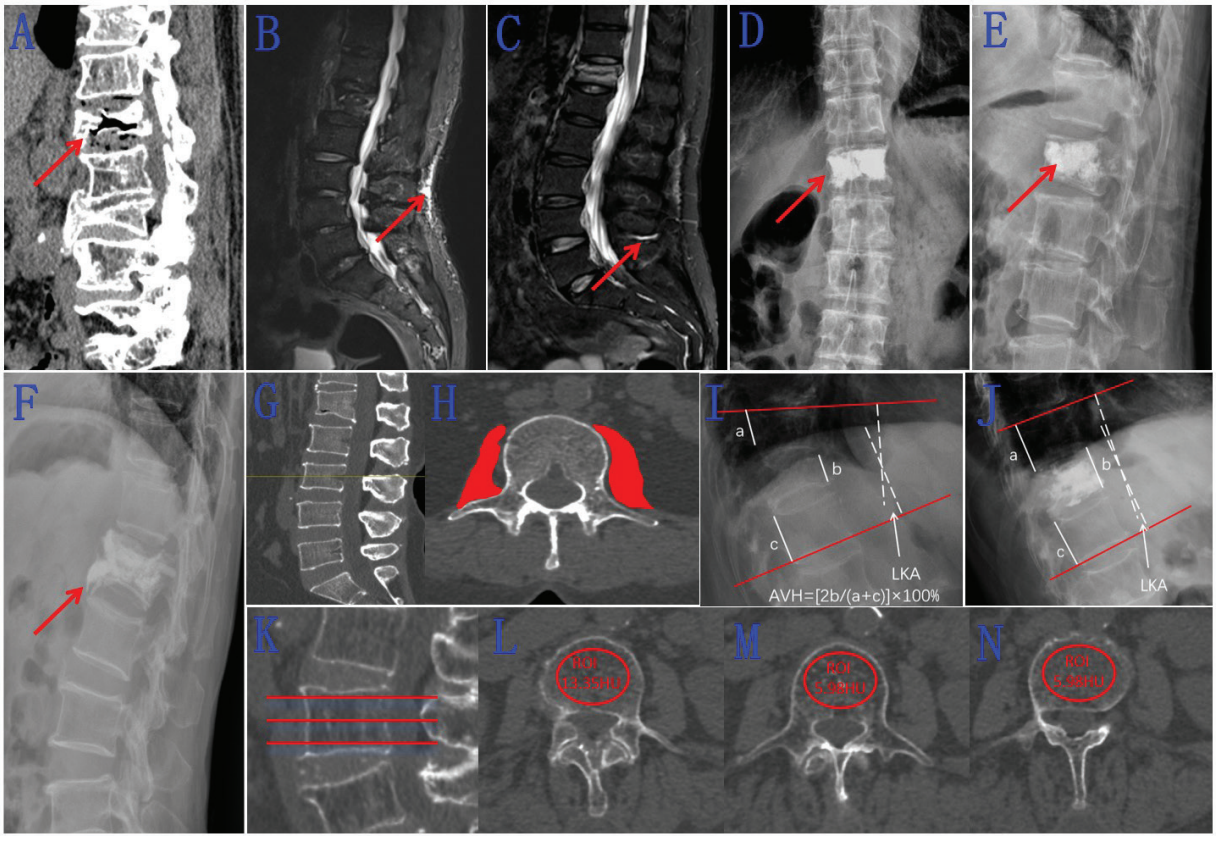

Fig. 1. *Definitions and measurement methods of various indicators. A: intravertebral vacuum cleft; B: posterior fascia oedema; C: interspinous ligament degeneration; D,E: bone cement distribution; F: bone cement leakage; G,H: sarcopenia; I,J: preoperative anterior vertebral height and Cobb angle; K–N: Hounsfield Unit value.*

ages and divided it by the square of the height (Total Psoas Area, TPA). Sarcopenia was diagnosed if the TPA was less than 385 mm²/m² for women or less than 545 mm²/m² for men (Figs. 1G, 1H).

AVH

AVH was calculated as the height of the anterior border of the fractured vertebra divided by the average posterior height of the adjacent vertebrae, multiplied by 100% (Figs. 1I, 1J).

Cobb Angle

We drew extension lines along the upper and lower endplates of the adjacent vertebrae and measured the angle formed by the perpendiculars to these lines (Figs. 1I, 1J).

HU Value

We measured the HU value on axial images of the L3 vertebra in 3 areas: just below the upper endplate, in the middle of the vertebral body, and just above the lower endplate. The average HU value was calculated from the largest possible elliptical region of interest (Figs. 1K–N).

Statistical Methods

Data Analysis

We used IBM SPSS Statistics 26.0 (IBM Corporation) for data analysis. A univariate analysis was conducted to identify potential risk factors for postoperative residual low back pain. For continuous variables following a normal distribution, data are presented as mean ± SD ($\bar{X}$ ± S) and compared between groups using the t test. For continuous variables not following a normal distribution, data are presented as the median (interquartile range) (M[Q1, Q3]) and compared using the rank-sum test. Categorical variables are expressed as frequency (n [%]) and compared using the χ^2 test.

Correlation Heatmap Analysis

A correlation heatmap was created to explore relationships between variables in the dataset. Pearson correlation coefficients were calculated for each pair of variables to quantify the strength and direction of their linear relationships. The heatmap provided a visual representation of these correlations, with darker shades indicating stronger correlations.

Data Processing

The "group" was set as the target variable. Patients were assigned to Group 0 if their DLP VAS score was ≥ 5 on the first postoperative day, and to Group 1 if the score was < 5. Categorical variables were converted into dummy variables, while continuous variables were standardized to enhance model performance. To address multicollinearity, the reduce VIF method was employed, leading to the removal of the "Cement Distribution_1" variable due to its high variance inflation factor value. Additionally, to resolve class imbalance, the Synthetic Minority Oversampling Technique was applied to balance the dataset. The data were then split into training and test sets in a 7:3 ratio, providing a solid foundation for robust model evaluation.

Model Training

After data preprocessing, a random forest classifier was chosen due to its strength in handling small datasets. Grid search with cross-validation was used for hyperparameter tuning, exploring combinations of the number of estimators, maximum depth, and maximum features. The optimal configuration determined 6 estimators, a maximum depth of 7, and a maximum of 6 features per split. Model performance was evaluated using a confusion matrix, which provided key metrics such as accuracy, precision, recall, and the F1 score, offering a detailed view of classification performance. Moreover, feature importance was analyzed based on the random forest's ability to rank variables according to their contribution to the prediction, offering insights into the most significant factors.

Results

A total of 179 patients with complete data were included in the study (mean [SD] age: 71.41 [7.76] years; 149 women). Among them, 5 patients had T10 fractures, 6 had T11 fractures, 47 had T12 fractures, 71 had L1 fractures, and 50 had L2 fractures. A total of 23 characteristic variables were included in the study.

Patients without postoperative DLP were categorized into Group 0 (150 patients; 128 women). Patients with postoperative DLP were assigned to Group 1 (29 patients; 21 women).

Detailed characteristic values for both groups are presented in Fig. 2. The results of the univariate analysis indicated no significant differences in preoperative baseline characteristics between the 2 groups (Table 1; $P > 0.05$). Both groups showed a significant reduction in postoperative VAS and ODI scores compared to preoperative values, but Group 1 had significantly lower

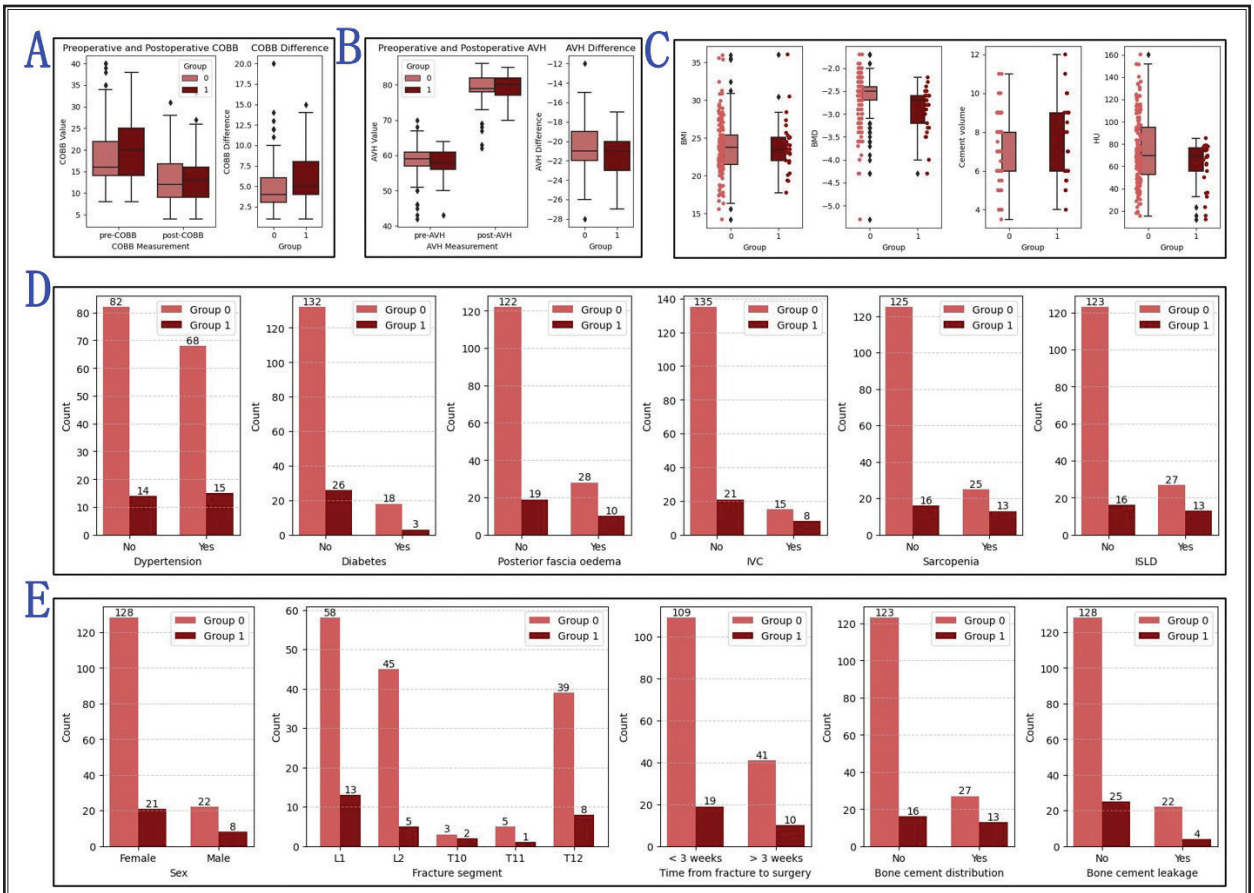

Fig. 2. *The general data of the two groups. A: preoperative, postoperative Cobb angles and difference by group; B: preoperative, postoperative anterior vertebral height and difference by group; C: distribution for body mass index, bone mineral density, bone cement volume, Hounsfield Unit by group; D: distribution for hypertension, diabetes, thoracolumbar fascia injury, intravertebral vacuum cleft, sarcopenia, interspinous ligament degeneration; E: distribution for gender, fracture segment, time from fracture to surgery, bone cement distribution, bone cement leakage.*

postoperative VAS and ODI scores compared to Group 0; these differences were statistically significant (Table 1; $P < 0.05$). Additionally, significant differences were observed between the 2 groups in terms of BMD, IVC, sarcopenia, bone cement distribution, ISLD, and HU values (Table 1; $P < 0.05$).

The correlation heatmap analysis revealed a moderate correlation between DLP and both sarcopenia and ISLD, with each correlation coefficient being approximately 0.25 (Fig. 3A). After selecting the optimal hyperparameters, a random forest model was employed to predict the target variable on the test dataset. Key classification metrics derived from the confusion matrix were used to assess the model's performance. The results showed strong performance across all key metrics, with an accuracy of 91.67%, precision of 92.11%, recall of 91.67%, and an F1 score of 91.66% (Fig. 3B).

The random forest algorithm ranked the features based on their contribution to predictive accuracy, highlighting the top 20 most important features (Fig. 3C). The feature importance chart indicated that the preoperative Cobb angle and sarcopenia are the most crucial features, with importance scores of approximately 0.15 and 0.10, respectively. These 2 features alone accounted for nearly half of the model's decision-making power. Age and ISLD also demonstrated significant contributions, with importance scores of around 0.09. Other key variables included BMD, PFO, bone cement distribution, and HU values, each with an importance score ranging from 0.05 to 0.10, indicating a moderate effect on the predictions.

Table 1. *Comparison of general data of patients with osteoporotic vertebral compression fractures in the Nonpain Group (Group 0) and the Pain Group (Group 1).*

	Group 0 (n = 150)	Group 1 (n = 29)	*P*
Gender (%)			0.106
Men	22 (14.67)	8 (27.59)	
Women	128 (85.33)	21 (72.41)	
Age, mean (SD)	71.19 ± 7.59	72.52 ± 7.80	0.402
Fracture segment (%)			0.131
T10	3 (2.00)	2 (6.90)	
T11	5 (3.33)	1 (3.45)	
T12	39 (26.00)	8 (27.59)	
L1	58 (38.66)	13 (44.83)	
L2	45 (30.00)	5 (17.24)	
Body mass index (kg/m^2)	23.81 ± 3.69	23.96 ± 3.60	0.833
Bone mineral density	-2.64 ± 0.53	-2.88 ± 0.50	0.027
Hypertension (%)			0.528
Yes	82 (54.67)	14 (48.28)	
No	68 (45.33)	15 (51.72)	
Diabetes (%)			0.797
Yes	132 (88.00)	26 (89.66)	
No	18 (12.00)	3 (10.34)	
Time from fracture to surgery (%)			0.435
< 3Weeks	109 (72.67)	19 (65.52)	
≥ 3Weeks	41 (27.33)	10 (34.48)	
PFO (%)			0.057
Yes	122 (81.33)	19 (65.52)	
No	28 (18.67)	10 (34.48)	
IVC (%)			0.018
Yes	135 (90.00)	21 (72.41)	
No	15 (10.00)	8 (27.59)	
Sarcopenia (%)			< 0.01*
Yes	125 (83.33)	16 (55.17)	
No	25 (16.67)	13 (44.83)	
Bone cement distribution (%)			< 0.01*
Yes	123 (82.00)	16 (55.17)	
No	27 (18.00)	13 (44.83)	
Bone cement leakage (%)			0.902
Yes	128 (85.33)	25 (86.21)	
No	22 (14.67)	4 (13.79)	
ISLD (%)			< 0.01*
Yes	123 (82.00)	16 (55.17)	
No	27 (18.00)	13 (44.83)	
Cement volume (mean ± SD)	6.98±1.55	7.19±1.99	0.589

Table 1 cont. *Comparison of general data of patients with osteoporotic vertebral compression fractures in the Nonpain Group (Group 0) and the Pain Group (Group 1).*

	Group 0 (n = 150)	Group 1 (n = 29)	*P*
Preoperative Cobb angle (mean±SD)	18.28 ± 6.81	19.93 ± 7.38	0.240
Postoperative Cobb angle	13.33 ± 5.50	14.07 ± 6.98	0.526
Preoperative AVH (mean ± SD)	53.53 ± 4.41	57.83 ± 4.47	0.437
Postoperative AVH	79.07 ± 3.96	79.24 ± 3.63	0.832
Preoperative VAS (mean ± SD)	7.27 ± 0.96	7.38 ± 1.01	0.591
One day postoperative VAS	2.35 ± 0.62	4.59 ± 0.68	< 0.01*
One month postoperative VAS (mean ± SD)	1.59 ± 0.59	2.31 ± 0.54	< 0.01*
3month postoperative VAS	1.18 ± 0.63	1.72 ± 0.59	< 0.01*
Preoperative ODI (mean ± SD)	71.80 ± 2.89	71.93 ± 2.90	0.824
One day postoperative ODI	31.49 ± 2.09	34.41 ± 2.75	< 0.01*
One month postoperative ODI (mean ± SD)	19.93 ± 1.86	21.83 ± 2.44	< 0.01*
3 month postoperative ODI	10.33 ± 1.61	11.79 ± 2.16	< 0.01*
HU	74.50 ± 30.74	62.22 ± 20.59	0.01

PFO: posterior fascia oedema; IVC: intravertebral vacuum cleft; ISLD: interspinous ligament degeneration; AVH: anterior vertebral height; VAS: Visual Analog Scale; ODI: Oswestry Disability Index; HU: Hounsfield Unit. *$P < 0.05$

Discussion

OVCF is a common orthopedic condition in the elderly; typical clinical symptoms include localized fracture pain or DLP. Persistent pain and functional limitations significantly reduce the quality of life for these patients (15,16).

PKP is an effective treatment for OVCF. It alleviates pain, improves quality of life, and reduces mortality rates in affected individuals. However, some patients experience unresolved DLP, leading to a loss of confidence in the procedure and further decreasing their quality of life (17,18).

Studies have shown that intraoperative interventions, such as local facet joint blocks or corticosteroid injections, can effectively reduce the incidence of post-PKP DLP. However, postsurgical DLP only occurs in some

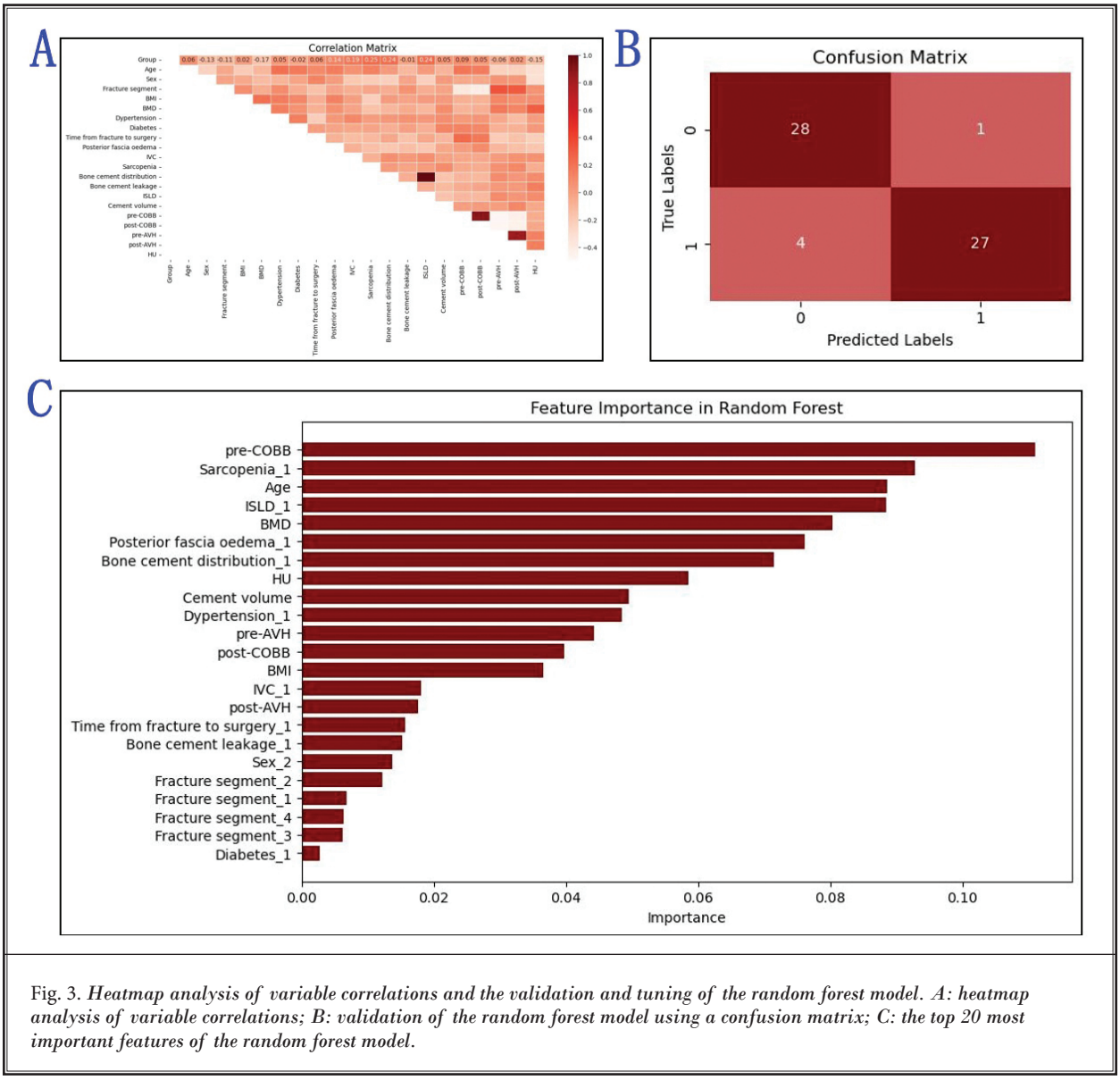

Fig. 3. *Heatmap analysis of variable correlations and the validation and tuning of the random forest model. A: heatmap analysis of variable correlations; B: validation of the random forest model using a confusion matrix; C: the top 20 most important features of the random forest model.*

cases (16.2% of patients in our study), and treating all patients with additional interventions remains debatable. Numerous predictive models have been developed to identify factors associated with post-PKP DLP (9-11,18). Nevertheless, these studies primarily focus on identifying potential risk factors but did not explore the relative importance and specific roles of these factors in predicting postoperative pain. Further research is needed to accurately assess the contribution of each risk factor in determining postsurgical DLP.

AI has seen rapid advancements in medicine recently, particularly in areas such as imaging analysis, disease diagnosis, and personalized treatment. AI can integrate a variety of clinical information from patients, such as medical history, physical exam findings, lab data, and imaging results to generate individualized diagnostic plans (19-21). Additionally, machine learning algorithms based on big data can identify individual differences among patients, especially when considering the coexistence of multiple conditions in the elderly, such as diabetes and hypertension. AI can analyze disease-related risk factors, optimize diagnostic processes, and accurately and quickly predict the onset of related diseases, ultimately enabling a fast diagnosis and personalized treatment.

In our study, we first collected demographic factors, comorbidities, clinical symptoms, laboratory data, and imaging data from patients with OVCF who underwent PKP. Based on whether patients experienced postoperative DLP, they were divided into 2 groups for a univariate analysis of the risk factors associated with this complication. The results showed significant differences between the 2 groups in terms of BMD, IVC, sarcopenia, bone cement distribution, ISLD, and HU values. Osteoporosis is closely related to lower back pain, and BMD and HU values are important indicators of osteoporosis. Patients with lower BMD are more likely to experiencing DLP (22,23).

Our study found that decreased BMD is a risk factor for post-PKP DLP. However, this association may not have clinical significance. This is because BMD measurement is based on the average bone density of the lumbar spine (L1-L4), while OVCF typically occurs in the T10-L2 region, and the fracture itself can interfere with the BMD results. Therefore, even though univariate analysis indicates low BMD as a risk factor for postsurgical DLP, it cannot be used as a clinical predictor. Thus, our study employed HU values as a predictor for this complication.

Additionally, our research found that heatmap analysis of variable correlations indicated a moderate correlation (about 0.25) between sarcopenia and ISLD with postsurgical DLP. This suggests that these factors may play a role in predicting postoperative pain.

The random forest model consists of numerous decision trees, each running independently of the others, making this model particularly suitable for smaller datasets (23,24). Our study had 179 patients and 23 features, making the random forest model more appropriate for predicting risk factors. Additionally, the random forest model can provide importance scores for each variable, allowing us to evaluate the role of each variable in classification. After building the random forest model, key classification metrics derived from the confusion matrix were used to assess the model's performance. The results show that the model performed strongly across all key metrics. The high precision indicates that the model is very effective at minimizing false positives, while the similar recall value suggests it successfully identified most of the actual positive cases.

The F1 score balances precision and recall, further confirming the model's reliability and balance in classification, making it particularly suitable for situations where minimizing both false positives and false negatives is crucial. The feature importance ranking of the random forest algorithm, based on their contribution to prediction accuracy, is as follows: preoperative Cobb angle, sarcopenia, age, ISLD, BMD, PFO, bone cement distribution, and HU value.

To some extent, the results from the random forest model align with the findings of univariate analysis and the variable correlation heatmap. However, it is important to note that the random forest model identified the preoperative Cobb angle as a risk factor, which was missed by univariate analysis and the variable correlation heatmap. The preoperative Cobb angle can assess the condition of the vertebrae and surrounding soft tissue damage; a smaller angle indicates more severe vertebral fractures and associated soft tissue damage, which may be a significant cause of postoperative DLP.

Another aspect we need to address is that all 3 models predicted that sarcopenia and ISLD are risk factors for post-PKP DLP. Sarcopenia refers to the progressive deterioration of muscle function due to the loss of skeletal muscle mass, with an incidence rate of 24%–56% among patients older than 60. Among elderly patients undergoing orthopedic surgery, 44% suffer from sarcopenia. It is a known risk factor for falls, fractures, disability, and increased postoperative morbidity and mortality (25). Chen, et al (26) reported that, compared to patients without sarcopenia, those with sarcopenia who underwent surgery for lumbar degenerative diseases showed less improvement in functional ability, quality of life, physical health, and pain relief, and had longer hospital stays. We consider that patients with sarcopenia may have insufficient lumbar and back muscle strength, and while PKP surgery can restore spinal stability, the process of getting out of bed and moving still requires coordination of the lumbar muscles.

Poor lumbar muscle strength in patients with sarcopenia may be a significant reason for postsurgical DLP. The interspinous ligament is a key component of the posterior ligamentous complex and plays an indispensable role in the stability of the thoracolumbar spine (27-29). When an OVCF occurs, the compensatory ability of the interspinous ligament, which is already degenerated, is reduced, making it more prone to injury. Minor injuries to the interspinous ligament may not be detectable by magnetic resonance imaging, which could explain why ISLD leads to post-PKP DLP.

Our study has some limitations. It is a single-center retrospective study, including only patients with OVCF who underwent PKP surgery—this may have introduced selection and recall bias. Additionally, the overall sample size was relatively small, and the follow-up pe-

riod was short. In the future, we plan to prospectively include more patients with OVCF and incorporate more research variables to better assist in treating pain distant from the fracture site in clinical settings.

Conclusion

For DLP related to OVCF, the introduction of AI provides clinicians with a new tool. Our random forest model performed strongly across all key metrics and can effectively predict post-PKP DLP in patients with OVCF. This model can provide precise guidance for selecting treatment plans for patients with OVCF undergoing PKP surgery.

References

1. Ong KL, Beall DP, Frohbergh M, Lau E, Hirsch JA. Were VCF patients at higher risk of mortality following the 2009 publication of the vertebroplasty "sham" trials? *Osteoporos Int* 2018; 29:375-383.
2. Hirsch JA, Chandra RV, Carter NS, Beall D, Frohbergh M, Ong K. Number needed to treat with vertebral augmentation to save a life. *AJNR Am J Neuroradiol* 2020; 41:178-182.
3. Hinde K, Maingard J, Hirsch JA, Phan K, Asadi H, Chandra RV. Mortality outcomes of vertebral augmentation (vertebroplasty and/or balloon kyphoplasty) for osteoporotic vertebral compression fractures: A systematic review and meta-analysis. *Radiology* 2020; 295:96-103.
4. Li Q, Wang S, Wang Q, Yan P, Yang J. Percutaneous kyphoplasty through unilateral puncture on the convex side for the treatment of painful osteoporotic vertebral compression fracture with scoliosis. *BMC Musculoskelet Disord* 2024; 25:294.
5. Li Y, Feng X, Pan J, et al. Percutaneous vertebroplasty versus kyphoplasty for thoracolumbar osteoporotic vertebral compression fractures in patients with distant lumbosacral pain. *Pain Physician* 2021; 24:E349-E356.
6. Niu J, Song D, Gan M, et al. Percutaneous kyphoplasty for the treatment of distal lumbosacral pain caused by osteoporotic thoracolumbar vertebral fracture. *Acta Radiol* 2018; 59:1351-1357.
7. Li QD, Yang JS, Gong HL, et al. Can additional facet joint block improve the clinical outcome of kyphoplasty for acute osteoporotic vertebral compression fractures? *Pain Physician* 2021; 24:283-291.
8. Lin F, Zhang Y, Wu T, et al. Local anesthetic and steroid injection to relieve the distal lumbosacral pain in osteoporotic vertebral compression fractures of patients treated with kyphoplasty. *Pain Physician* 2022; 25:E581-E587.
9. Lin M, Wen X, Huang Z, et al. A nomogram for predicting residual low back pain after percutaneous kyphoplasty in osteoporotic vertebral compression fractures. *Osteoporos Int* 2023; 34:749-762.
10. Inose H, Kato T, Ichimura S, et al. Predictors of residual low back pain after acute osteoporotic compression fracture. *J Orthop Sci* 2021; 26:453-458.
11. Yu H, Luo G, Wang Z, Yu B, Sun T, Tang Q. Predictors of residual low back pain in patients with osteoporotic vertebral fractures following percutaneous kyphoplasty. *Front Surg* 2023; 10:1119393.
12. Biamonte E, Levi R, Carrone F, et al. Artificial intelligence-based radiomics on computed tomography of lumbar spine in subjects with fragility vertebral fractures. *J Endocrinol Invest* 2022; 45:2007-2017.
13. Granata V, Fusco R, Coluccino S, et al. Preliminary data on artificial intelligence tool in magnetic resonance imaging assessment of degenerative pathologies of lumbar spine. *Radiol Med* 2024; 129:623-630.
14. Wang P, Zhang Z, Xie Z, et al. Natural language processing-driven artificial intelligence models for the diagnosis of lumbar disc herniation with L5 and S1 radiculopathy: A preliminary evaluation. *World Neurosurg* 2024; 189:e300-e309.
15. Mitani K, Takahashi T, Tokunaga S, et al. Therapeutic prediction of osteoporotic vertebral compression fracture using the AO Spine-DGOU Osteoporotic Fracture Classification and classification-based score: A single-center retrospective observational study. *Neurospine* 2023; 20:1166-1176.
16. Patel D, Liu J, Ebraheim NA. Managements of osteoporotic vertebral compression fractures: A narrative review. *World J Orthop* 2022; 13:564-573.
17. Manji R, Ponzano M, Ashe MC, et al. Exploring the association between pain and fracture characteristics in women with osteoporotic vertebral fractures. *Physiother Can* 2022; 74:165-172.
18. Zhang Z, Zhang Y, Li L, et al. Risk factors for low back pain following percutaneous vertebroplasty in patients with osteoporotic vertebral compression fracture. *Am J Transl Res* 2024; 16:3778-3786.
19. Liawrungrueang W, Park JB, Cholamjiak W, Sarasombath P, Riew KD. Artificial intelligence-assisted MRI diagnosis in lumbar degenerative disc disease: A systematic review. *Global Spine J* 2024:21925682241274372.
20. Saravi B, Zink A, Ülkümen S, Couillard-Despres S, Lang G, Hassel F. Artificial intelligence-based analysis of associations between learning curve and clinical outcomes in endoscopic and microsurgical lumbar decompression surgery. *Eur Spine J* 2023; 33:4171-4181.
21. Sui H, Gong Y, Liu L, et al. Comparison of artificial intelligence-assisted compressed sensing (ACS) and routine two-dimensional sequences on lumbar spine imaging. *J Pain Res* 2023; 16:257-267.
22. Wang H, Huang J, Tao L, Liu D, Song C. Efficacy and safety of minodronate in the treatment of postmenopausal osteoporosis with low back pain: A single-centre, randomized and open-label controlled trial. *Trials* 2024; 25:534.
23. Umesh M, Ethiraj P, Nazar SM, Agarawal S, Shanthappa AH. Does zoledronic acid provide a good clinical outcome in patients with chronic back pain associated with vertebral osteoporosis? *Cureus* 2023; 15:e33328.
24. Wang H, Wang Y, Li Y, Wang C, Qie S. A diagnostic model of nerve root

compression localization in lower lumbar disc herniation based on random forest algorithm and surface electromyography. *Front Hum Neurosci* 2023; 17:1176001.

25. Gaddikeri MB, Nene A, Patel P, Bamb H, Bhaladhare S. Sarcopenia and its effects on outcome of lumbar spine surgeries. *Eur Spine J* 2024; 33:1369-1380.
26. Chen MJ, Lo YS, Lin CY, et al. Impact of sarcopenia on outcomes following lumbar spine surgery for degenerative disease: An updated systematic review and meta-analysis. *Eur Spine J* 2024; 33:3369-3380.
27. Iwanaga J, Simonds E, Yilmaz E, Schumacher M, Patel M, Tubbs RS. Anatomical and biomechanical study of the lumbar interspinous ligament. *Asian J Neurosurg* 2019; 14:1203-1206.
28. Creighton A, Sanguino RA, Cheng J, Wyss JF. Successful treatment of supraspinous and interspinous ligament injury with ultrasound-guided platelet-rich plasma injection: Case series. *HSS J* 2021; 17:227-230.
29. Zhang JF, Liu C, Yu HJ, Ma JJ, Cai HX, Fan SW. Degenerative changes in the interspinous ligament. *Acta Orthop Traumatol Turc* 2014; 48:661-666.